Electronic supplementary information

High-Performance Wide-Bandgap Copolymers Based on Indacenodithiophene and indacenodithieno[3,2-b]thiophene Units

Yunhao Cai,[‡a] Xiaolong Zhang,[‡a] Xiaonan Xue,[a] Donghui Wei,[b] Lijun Huo,*[a] and Yanming Sun*[a]

[a]*School of Chemistry, Beihang University, Beijing 100191, P. R. China. *E-mail: huolijun@buaa.edu.cn; sunym@buaa.edu.cn*

[b]*The College of Chemistry and Molecular Engineering, Zhengzhou University, Zhengzhou, Henan Province 450001, P. R. China.*

Instruments and measurements

Atomic force microscopy (AFM) images were obtained using a NanoMan VS microscope in the tapping mode. UV–vis absorption measurements were performed on a Hitachi (model U-3010) UV–vis spectrophotometer. Cyclic voltammetric (CV) measurements were carried out in a conventional three-electrode cell using a Pt plate as the working electrode, Pt wire as the counter electrode, and Ag/Ag+ electrode as the reference electrode on a Zahner IM6e Electrochemical Workstation in a tetrabutylammonium hexafl uorophosphate (Bu_4NPF_6) (0.1 M) acetonitrile solution at a scan rate of 20 mV s^{-1} . In UV-vis absorption measurement, we used a Hitachi (model U-3010) UV-vis spectrophotometer. We adopted a Keithley 4200 semiconductor parametric analyzer to characterize electrical properties. The OSCs performance were measured by an Air Mass 1.5 Global (AM 1.5 G) solar simulator (Class AAA solar simulator, Model 94063A, Oriel) with an intensity of 100 mW cm^{-2}, which was measured by a calibrated silicon solar cell and a readout meter (Model 91150V, Newport). The external quantum efficiency (IPCE) was recorded by a QEX10 Solar cell EQE measurement system (PV measurement, Inc).

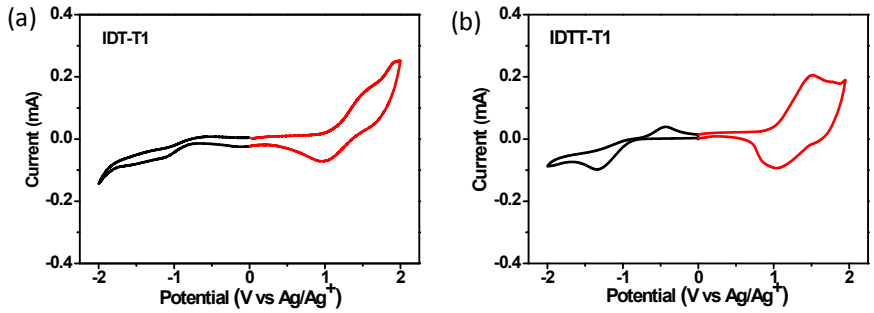

Figure S1. The electrochemical cyclic voltammetry measurements of IDT-T1 and IDTT-T1 films on a platinum electrode in acetonitrile solution containing 0.1 M Bu_4NPF_6 at a scan rate of 20 mV s^{-1}.

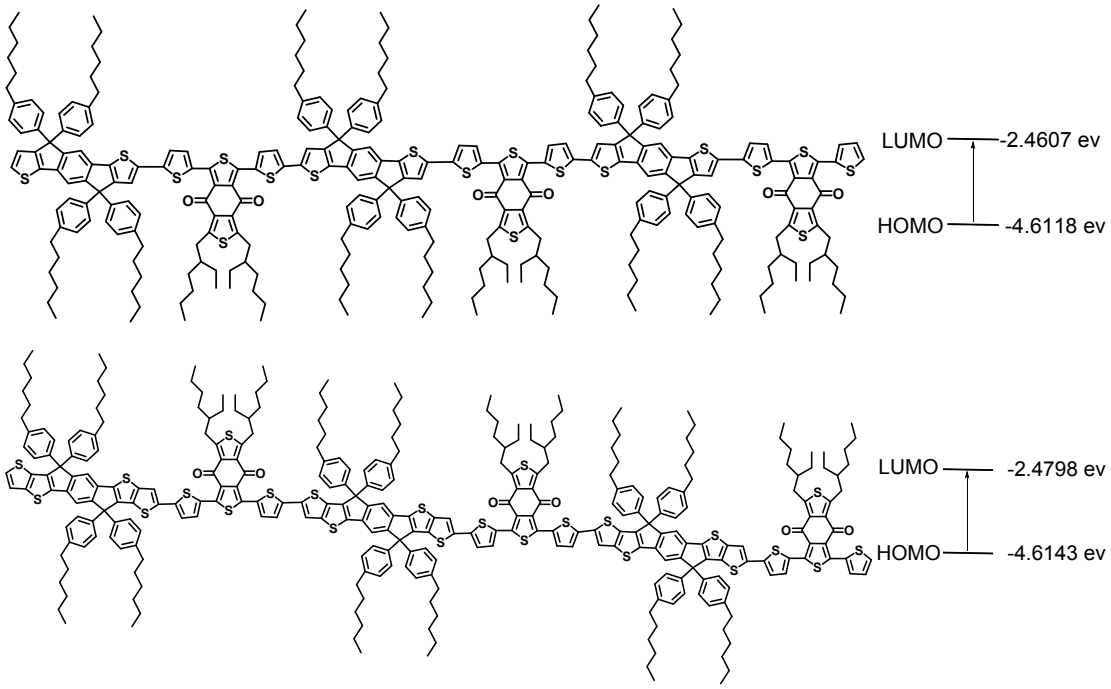

Figure S2. Theory calculated model molecule and its simulated energy levels of IDT-T1 using density functional theory (DFT) at the B3LYP/6-31G(d,p) level.

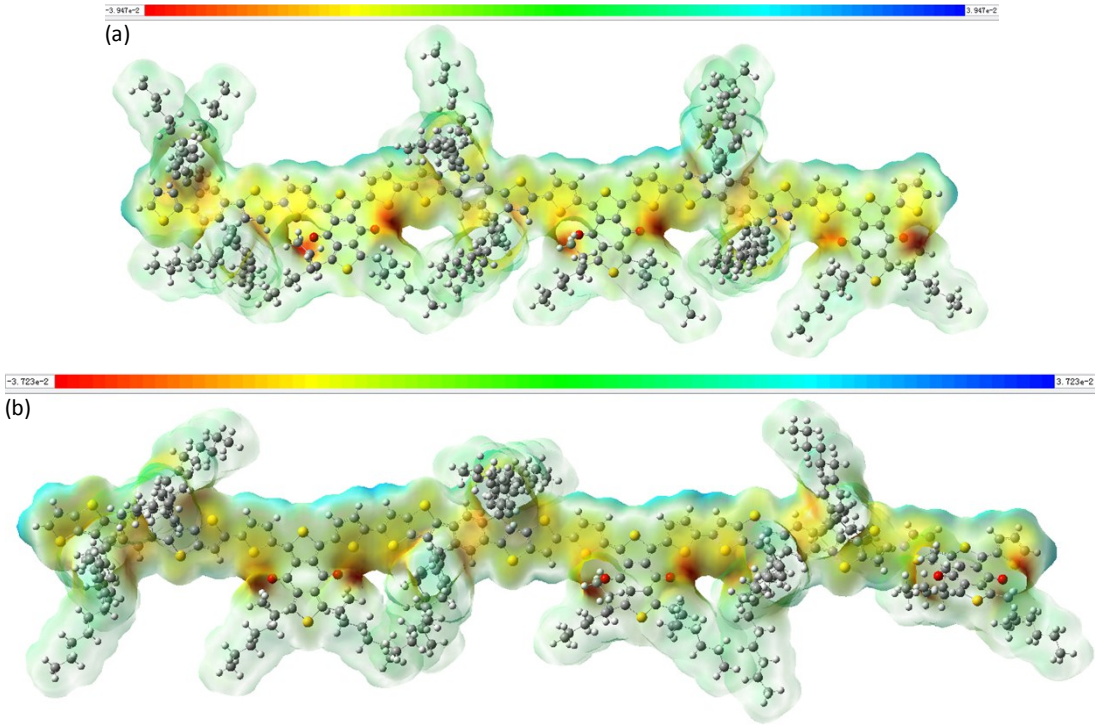

Figure S3. Maps of the DFT electrostatic potential (ESP) surfaces of a) IDT-T1 and b) IDTT-T1, red color indicates greater negative charge, while blue color indicates greater positive charge.

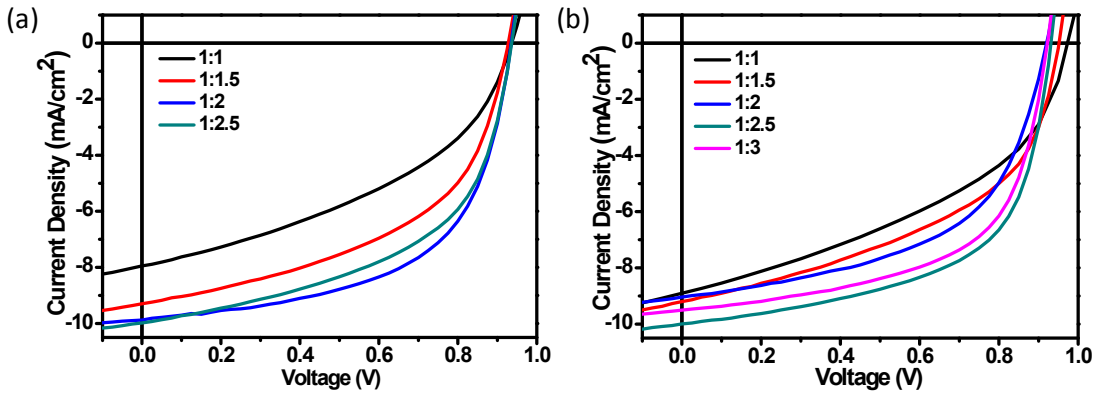

Figure S4. *J–V* curves of (a) IDT-T1:$PC_{71}BM$ (b) IDTT-T1: $PC_{71}BM$ solar cells with different weight ratios (w/o additive).

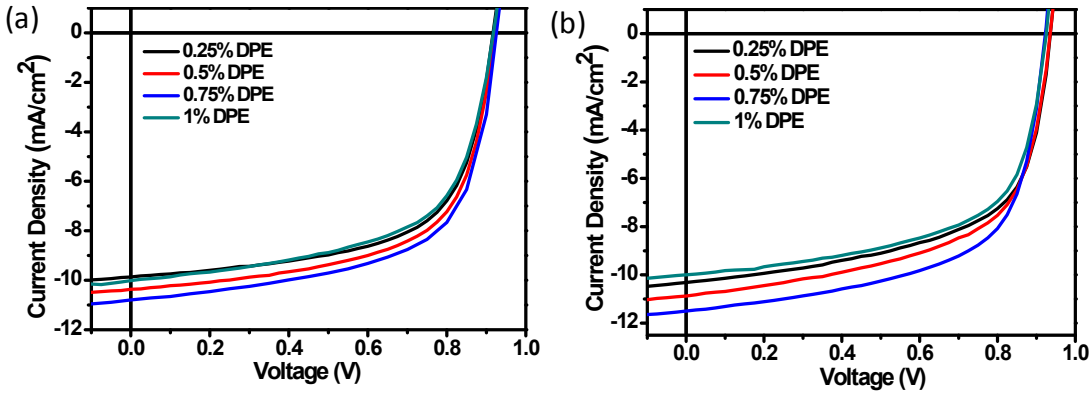

Figure S5. *J–V* characteristics of (a) IDT-T1:$PC_{71}BM$ (b) IDTT-T1: $PC_{71}BM$ solar cells with different DPE concentrations.

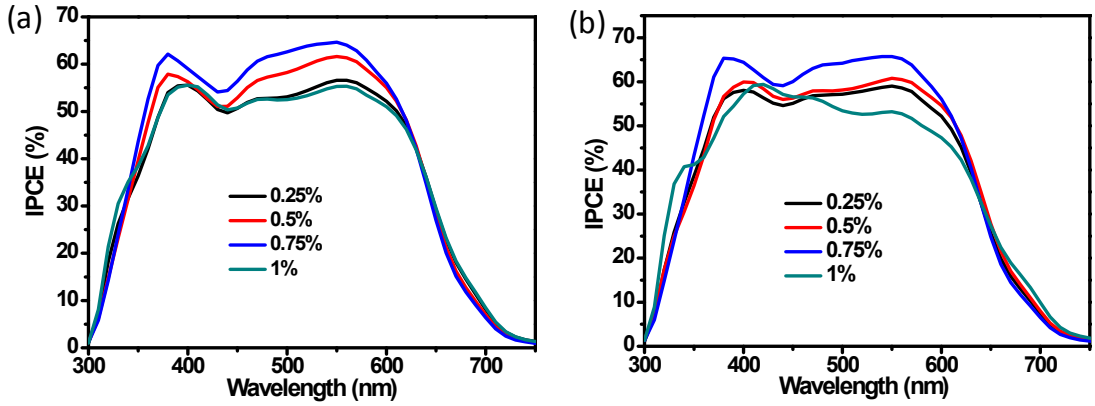

Figure S6. IPCE spectra of (a) IDT-T1:$PC_{71}BM$ (b) IDTT-T1: $PC_{71}BM$ solar cells with different DPE concentrations.

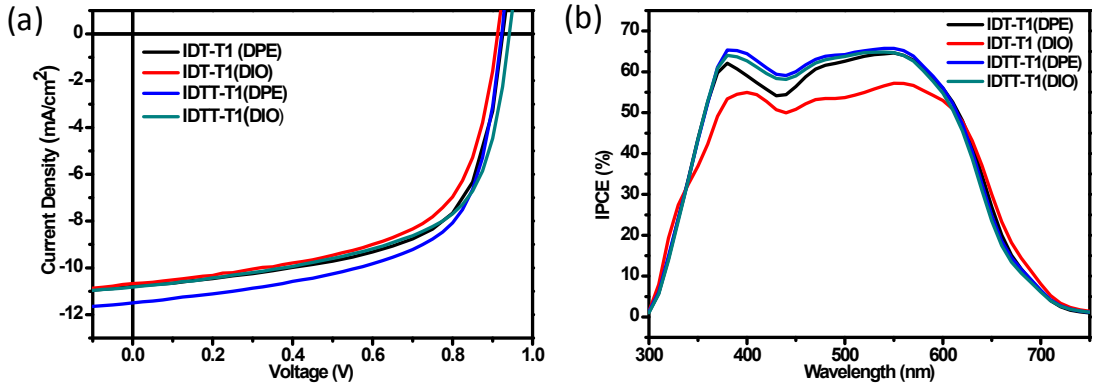

Figure S7. (a) *J–V* characteristics of IDT-T1:$PC_{71}BM$ and IDTT-T1:$PC_{71}BM$ solar cells with DPE or DIO additive. (b) IPCE spectra of IDT-T1:$PC_{71}BM$ and IDTT-T1:$PC_{71}BM$ solar cells with DPE or DIO additive.

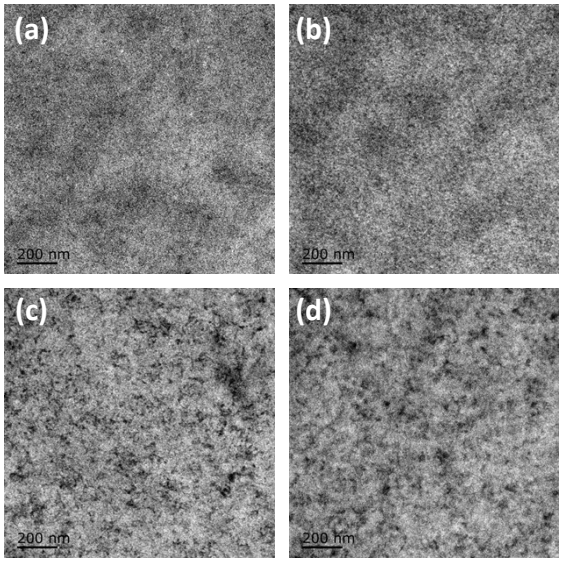

Figure S8. TEM images of (a) IDT-T1:$PC_{71}BM$ blend film (b) IDT-T1:$PC_{71}BM$ blend film with 0.75% DPE (c) IDTT-T1:$PC_{71}BM$ blend film (d) IDTT-T1:$PC_{71}BM$ blend film with 0.75% DPE.

Table S1. Summarized device parameters of IDT-T1:$PC_{71}BM$ solar cells with different blend ratios (w/o additive) under the illumination of AM1.5G, 100 mW cm^{-2}.

Weight ratios [v/v]	**V_{oc} (V)**	**J_{sc} (mA/cm^2)**	**FF (%)**	**PCE[(a)] (%)**	**PCE_{max} (%)**
1:1	0.93±0.004	7.84±0.19	41.7±0.95	3.05±0.08	3.14
1:1.5	0.93±0.007	9.06±0.37	49.8±1.33	4.19±0.10	4.33
1:2	0.94±0.003	9.76±0.13	58.1±1.07	5.30±0.06	5.37
1:2.5	0.92±0.015	9.76±0.25	54.1±0.69	4.87±0.10	4.95

Table S2. Summarized device parameters of IDTT-T1:$PC_{71}BM$ solar cells with different blend ratios (w/o additive) under the illumination of AM1.5G, 100 mW cm^{-2}.

Weight ratios [v/v]	**V_{oc} (V)**	**J_{sc} (mA/cm^2)**	**FF (%)**	**PCE$^{(a)}$ (%)**	**PCE_{max} (%)**
1:1	0.97±0.008	8.51±0.27	42.6±1.04	3.52±0.10	3.68
1:1.5	0.95±0.014	8.89±0.35	48.9±1.98	4.12±0.06	4.17
1:2	0.93±0.007	9.00±0.33	52.8±1.34	4.39±0.07	4.49
1:2.5	0.94±0.005	9.90±0.09	58.8±0.38	5.45±0.02	5.47
1:3	0.92±0.006	9.31±0.15	59.4±0.68	5.10±0.06	5.18

Table S3. Device parameters of OFETs based on IDT-T1.

	Annealing temperature [℃]	μ_{max} [$cm^2 V^{-1} s^{-1}$]	V_{th} [V]	I_{on}/I_{off}
IDT-T1 (BG-BC)	25	4.62×10^{-3}	5.15	9.12×10^{4}
	40	6.56×10^{-3}	-44.8	1.20×10^{5}
	50	5.46×10^{-3}	-6.71	1.01×10^{5}
	60	5.46×10^{-3}	-6.71	1.01×10^{5}
	70	8.04×10^{-3}	-46.8	1.19×10^{5}
	80	8.73×10^{-3}	-5.04	1.34×10^{5}
	90	8.86×10^{-3}	-3.21	1.40×10^{5}
	100	9.11×10^{-3}	-3.40	1.33×10^{5}
	110	9.81×10^{-3}	-5.03	9.45×10^{4}
	120	1.07×10^{-2}	-10.1	9.69×10^{4}
	130	1.49×10^{-2}	-18.5	9.69×10^{4}

	140	1.52×10^{-2}	-18.7	9.67×10^{4}
	150	2.05×10^{-2}	-27.1	7.31×10^{4}
	160	1.66×10^{-3}	-2.00	4.11×10^{4}
	170	1.30×10^{-3}	-1.63	1.72×10^{4}

Table S4. Device parameters of OFETs based on IDTT-T1.

	Annealing temperature [℃]	μ_{max} [$cm^2V^{-1}S^{-1}$]	V_{th} [V]	I_{on}/I_{off}
IDTT-T1 (BG-BC)	25	1.03×10^{-2}	7.11	2.51×10^{5}
	40	2.28×10^{-2}	-22.9	1.90×10^{6}
	50	3.82×10^{-2}	-35.9	1.31×10^{6}
	60	4.72×10^{-2}	-40.5	1.09×10^{6}
	70	5.75×10^{-2}	-45.8	9.10×10^{5}
	80	6.07×10^{-2}	-47.9	7.93×10^{5}
	90	6.30×10^{-2}	-39.7	8.50×10^{5}
	100	5.02×10^{-2}	-27.9	1.11×10^{5}
	110	5.38×10^{-2}	-31.3	6.86×10^{5}
	120	4.77×10^{-2}	-20.3	6.67×10^{5}
	130	5.26×10^{-2}	-17.5	6.82×10^{5}
	140	5.26×10^{-2}	-17.5	5.47×10^{5}
	150	6.91×10^{-2}	-22.5	3.43×10^{5}
	160	9.15×10^{-2}	-27.5	3.74×10^{5}

	170	1.13×10^{-1}	-29.3	4.45×10^{5}
	180	1.10×10^{-1}	-26.1	4.15×10^{5}
	190	9.44×10^{-2}	-26.0	3.80×10^{5}
	200	9.62×10^{-2}	-24.3	3.46×10^{5}
	210	8.13×10^{-2}	-21.4	2.58×10^{5}
	220	6.39×10^{-2}	-20.4	1.62×10^{5}
	230	4.45×10^{-2}	-17.5	8.77×10^{5}
	240	2.29×10^{-2}	-14.5	4.42×10^{4}
	250	1.39×10^{-2}	-13.1	1.92×10^{4}